

ANALYSIS OF PLANAR GRID OSCILLATORS

Scott C. Bundy

Zoya B. Popović

University of Colorado
 Department of Electrical and Computer Engineering
 Boulder, Colorado 80309

Abstract – A full-wave analysis of infinite periodic grid structures loaded with active devices is presented. The grid consists of arbitrary periodic metal patterns printed on one or both sides of a dielectric slab in free space. Since the structure is periodic, it is sufficient to analyze a single unit cell. An expression is derived relating the tangential electric field to the surface current density on the metal, which is determined by the method of moments. The driving-point impedances are found for any active devices embedded in the grid structure. Using this analysis, the metal geometry can be optimized for designing active quasi-optical power-combining grids in the microwave and millimeter-wave regions.

1 Introduction

Free-space power-combining techniques for the microwave and millimeter-wave regions demonstrated to date are: (1) grid oscillators and amplifiers [1, 2], and (2) active resonant antennas, such as patches or slots that incorporate oscillator or amplifier circuits [3, 4]. The largest number of combined devices was achieved in grid oscillators, in which a metal mesh loaded with up to 100 MESFETs was placed in a Fabry-Perot cavity [5]. This method was first proposed and the field modes theoretically investigated for the case of a confocal resonator with one planar mirror [6]. For a power-combiner design, it is convenient to use a circuit model in which the active device is embedded. A circuit model for which the elements were found using an EMF analysis was presented in [5]. This analysis is subject to certain approximations and cannot deal with an arbitrary metal geometry for the grid structure, but is adequate for grids in which the active device terminals are connected to thin metal strips [5]. However, as demonstrated in [7] by comparing a thin-strip grid oscillator with a bow-tie grid, the metal geometry significantly affects the behavior of the grid power combiners. Further, this work demonstrates the feasibility of quasi-optical systems consisting of grids printed on opposite sides of the same substrate, or stacked in each other's near fields. For example, in [7] a grid of varactor diodes was fabricated on the back side of a MESFET grid oscillator and demonstrated 10% electronic frequency tuning with less than 2 dB change in power.

The goal of the work presented in this paper is a design-oriented analysis of a generalized periodic active grid oscillator power combiner. The grid can have a three-terminal power-generating device on one side of an arbitrarily thick dielectric, and a control device such as a varactor or *pin* diode on the back side. Further, the shape of the grid metallization is arbitrary. To analyze the grid, a Fortran program was written for a personal computer based on full-wave theory and the results compared favorably with measurements and other theories for several well-known geometries.

2 Full-Wave Analysis of Loaded Periodic Grid Structures

A quasi-optical power-combining grid consists of an array of active devices which loads a periodic metal pattern printed on a dielectric substrate. In this analysis, it is assumed that the periodic grid structure is infinite in both the x and y directions, and that the solid-state devices operate in phase. Under these conditions, the behavior of the entire grid may be analyzed on the basis of a single unit cell, whose electric and magnetic wall boundaries arise from the symmetry of the currents in each unit cell. In the following analysis, arbitrary metallization is allowed on either one or both sides of the dielectric as long as the pattern is periodic and the unit cell boundary conditions are preserved. Figure 1 shows top and side views of a unit cell with metallization on both sides of the dielectric. For a grid oscillator, an active device is placed in the gap of the metal structure. To predict the behavior of the power combiner, it is important to know the

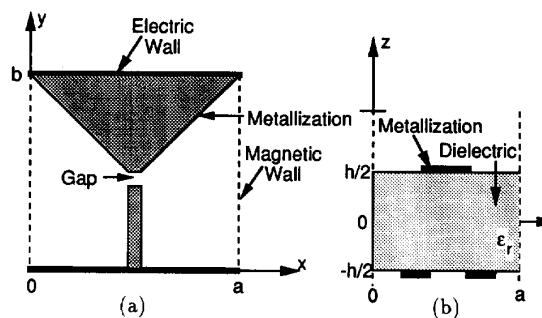
WE
3B

Figure 1: (a) Top view and (b) side view of a unit cell geometry with metallization on both sides of the dielectric.

driving-point impedance presented to the active device terminals. This impedance is determined by a full-wave analysis using the method of moments. An analytic relationship is first derived between the tangential electric field and the surface current density on both dielectric surfaces. A time-harmonic voltage generator representing the active device is placed in the gap, producing a constant electric field in the small region of the gap. The current on the metallization and in the gap is expanded as a summation of rooftop basis functions and Galerkin's moment method is applied to find the current. The ratio of the voltage across the gap to the current through the gap is the driving-point impedance seen by the device. This entire analysis is performed over a range of frequencies.

In power-combining grids demonstrated to date [1, 8], the active devices were transistors (MESFET, HEMT, or HBT) which are treated here as two-port devices. Therefore, there are two gaps in the metallization, one for each port, and the analysis is performed twice. First, gap 1 is driven with a generator with gap 2 short-circuited (metallized), and then gap 2 is driven with gap 1 metallized. Since the current on the entire structure is calculated for each case, two-port Y -parameters are readily determined. Two-port S -parameters (or any other desired parameters) may then be found from these Y -parameters, yielding a full, convenient

characterization of the grid geometry. This methodology can be extended to multi-port structures, such as a three-port voltage-controlled oscillator, in which a MESFET is located on the front-side metallization and a varactor diode on the back-side metallization as shown in Figure 2.

3 Prediction of Oscillation Frequency

In grid oscillators, once the grid geometry has been characterized, the resulting n -port network may be connected to appropriate circuit models for the active devices. Commercially available analysis software such as the Microwave Design System (MDS) by Hewlett-Packard may then be used to perform the linear or nonlinear analysis of the grid oscillator. The frequency of oscillation occurs where the open-loop gain of the circuit has magnitude greater than unity and zero phase. The S -parameters for the two different grid geometries shown in Figure 2 were computed by the above method. Identical devices (a Fujitsu MESFET on the front side and a varactor diode on the back side) were then connected to the two grids as shown in Figure 3, and the simulated open-loop gain for both cases is shown in Figure 4. The simulated oscillation frequency is 5.0 GHz for the grid with narrow-strip radiating elements and 6.3 GHz for the grid with approximated bow-tie radiating elements. It is clearly seen that the metal geometry itself significantly affects the operation of the grid oscillator. For characterizing the VCO performance, the loop gain was calculated for a different value of varactor diode capacitance in the approximated bow-tie grid. Changing the diode capacitance from 0.5 pF to 2.0 pF shifts the oscillation frequency from 6.3 GHz to 5.7 GHz, yielding a 10% tuning bandwidth for a 4:1 change in diode capacitance. This qualitatively agrees with the results in [7].

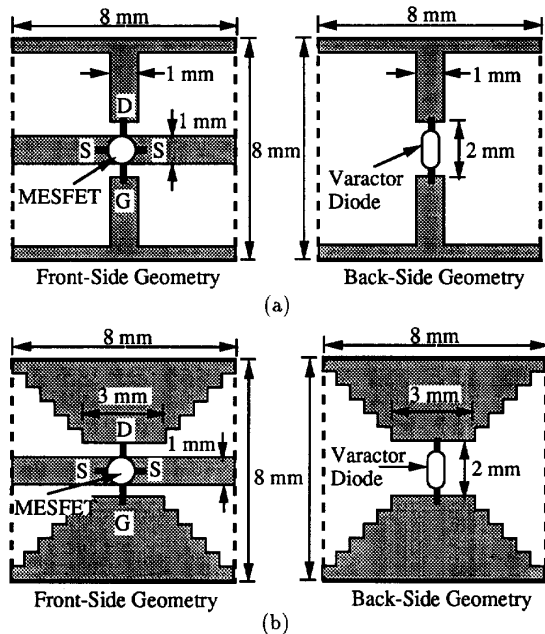


Figure 2: Two different grid oscillator geometries, (a) one with narrow-strip radiating elements and (b) another with approximated short bow-tie radiating elements. Both structures are printed on 1.5 mm thick substrates with $\epsilon_r = 2.2$. The MESFET metallization is on one side and the diode metallization on the other side of the dielectric substrate.

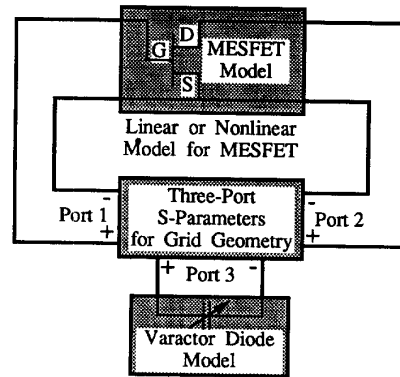


Figure 3: The circuit used by MDS to calculate the open-loop gain of the oscillator grids. Three-port S -parameters calculated using the full-wave analysis represent the grid geometry, a Curtice cubic model is used to represent the Fujitsu FLK052XV MESFET on the front-side metallization, and a simple 0.5 pF capacitor is used to model the reverse-biased varactor diode on the back-side metallization.

4 Reflection Coefficient Calculations

In addition to driving-point impedance calculations, it is also useful to calculate the reflection coefficient of passive periodic structures under normally incident plane wave illumination (eg., for quasi-optical filters used extensively in far-infrared applications). For passive structures there is no device driving the current on the metallization. Instead, a plane wave is assumed to be incident on the metal pattern in free space without the dielectric slab present. The current induced on the metal in turn re-radiates a reflected field. Since the tangential electric field on the metallization must be zero, the reflected electric field is used to determine the surface current density by the same technique discussed in Section 2. The TEM component of the re-radiated electric field is computed from the current distribution, and the reflection coefficient is then calculated. Transmission-line analysis is then used to include the effect of the dielectric slab. The metal pattern is modelled as a frequency-dependent shunt admittance which gives the same reflection coefficient in a 377Ω transmission line, and the dielectric is modelled as a transmission line of the appropriate characteristic impedance and length. Reflection and transmission coefficients of this circuit are then calculated.

A series of transmission coefficient measurements were performed using an HP 8510 network analyzer and two broadband horn antennas. The transmission coefficients of the structures were also computed using the full-wave analysis presented here as well as the moment method presented in [9]. First, an array of crossed dipoles was fabricated on my-

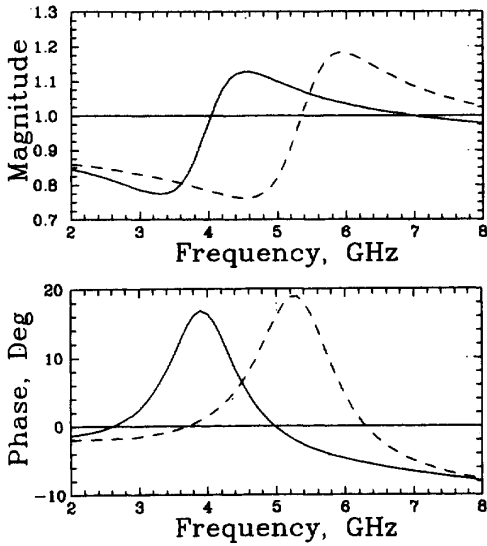


Figure 4: The magnitude and phase of the open-loop gain as calculated using MDS for two different grid geometries. The solid line corresponds to the geometry of Figure 2 (a) and the dashed line corresponds to the geometry of Figure 2 (b).

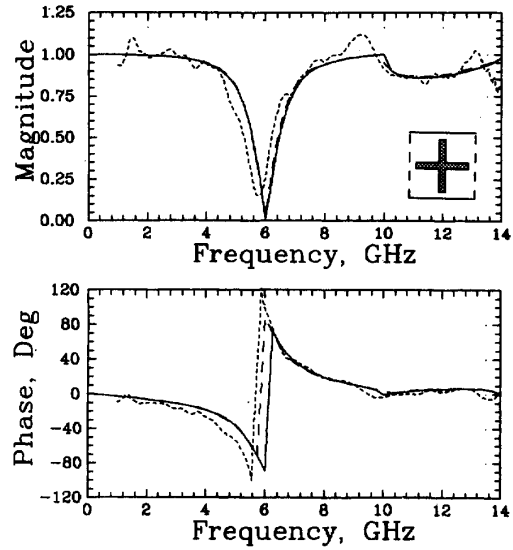


Figure 5: The transmission coefficient of an array of crossed dipoles. The solid line represents the full-wave theory presented here, the dashed line represents the theory presented in [9], the dotted line represents the measured results, and the unit cell of the structure is shown in the inset.

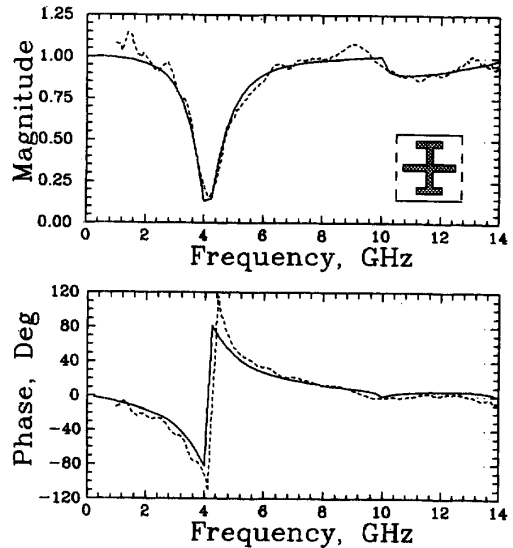


Figure 6: The transmission coefficient of an array of crossed dipoles with horizontal stubs on the vertical dipole element. The solid line represents the full-wave theory presented here, the dotted line represents the measured results, and the unit cell of the structure is shown in the inset.

lar and the comparison between measurement and theory is seen in Figure 5. The unit cell of this structure is shown as an inset in the figure. Then horizontal stubs were added on the end of the vertical dipole elements and the transmission coefficient results are shown in Figure 6. This pair of results indicates that the horizontal stubs placed on the end of the vertical dipole elements decrease the first resonant frequency of the structure from 6 GHz to 4 GHz. Finally, vertical stubs were added on the end of the horizontal dipole elements as well, resulting in an array of Jerusalem crosses. The transmission coefficients for this array are shown in Figure 7. The addition of these vertical stubs does not affect the first resonance, but it does introduce a rather broad frequency range over which most of the power is reflected. Even better agreement is seen for simple structures such as inductive and capacitive gratings.

5 Conclusion

A full-wave analysis of active quasi-optical grid oscillators is presented. The grid can have an arbitrary periodic metal pattern printed on either one or both sides of a dielectric. The analysis provides an embedding equivalent circuit for any multi-port active device loading the grid unit cell, and this circuit can then be analyzed using standard techniques. Two examples of MESFET grid oscillators backed by varactor grid tuning elements are presented and clearly show that the metal shape of the grid structure influences the oscillation frequency. As a verification of the method, transmission coefficients for several passive metal grids were

calculated and compared to measurement and other theories with good agreement. The theory can be extended to any periodic quasi-optical power combiner and should prove to be a useful tool in the design and optimization of these devices.

References

- [1] Z.B. Popović, M. Kim, and D.B. Rutledge, "Grid Oscillators," *International Journal of Infrared and Millimeter Waves*, Vol. 9, No. 7, 1988, pp. 647-654.
- [2] R.M. Weikle II, M. Kim, J.B. Hacker, M.P. DeLisio, Z.B. Popović, and D.B. Rutledge, "Transistor Oscillator and Amplifier Grids," *Proceedings of the IEEE*, Vol. 80, No. 11, Nov. 1992, pp. 1800-1809.
- [3] J. Birkeland and T. Itoh, "A 16-Element Quasi-Optical FET Oscillator Power-Combining Array with External Injection Locking," *IEEE Transactions on Microwave Theory and Techniques*, Vol. 40, No. 3, March 1992, pp. 475-481.
- [4] R.A. York and R.C. Compton, "Quasi-Optical Power Combining Using Mutually Synchronized Oscillator Arrays," *IEEE Transactions on Microwave Theory and Techniques*, Vol. 39, No. 6, June 1991, pp. 1000-1009.
- [5] Z.B. Popović, R.M. Weikle II, M. Kim, and D.B. Rutledge, "A 100-MESFET Planar Grid Oscillator," *IEEE Transactions on Microwave Theory and Techniques*, Vol. 39, No. 2, Feb. 1991, pp. 193-200.
- [6] J.W. Mink, "Quasi-Optical Power Combining of Solid-State Millimeter-Wave Sources," *IEEE Transactions on Microwave Theory and Techniques*, Vol. 34, No. 2, Feb. 1986, pp. 273-279.
- [7] S.C. Bundy, T.B. Mader, and Z.B. Popović, "Quasi-Optical Array VCOs," *IEEE Microwave Theory and Techniques Symposium Digest*, paper RR-5, June 1992, pp. 1539-1542.
- [8] E.A. Sovero, M. Kim, R.M. Weikle II, D.S. Deakin, W.J. Ho, J.A. Higgins, and D.B. Rutledge, "A Monolithic 35 GHz HBT Quasi-Optical Grid Oscillator," *GaAs IC Symposium*, 1992, pp. 305-308.
- [9] C.H. Tsao and R. Mittra, "Spectral-Domain Analysis of Frequency Selective Surfaces Comprised of Periodic Arrays of Cross Dipoles and Jerusalem Crosses," *IEEE Transactions on Antennas and Propagation*, Vol. 32, No. 5, May 1984, pp. 478-486.

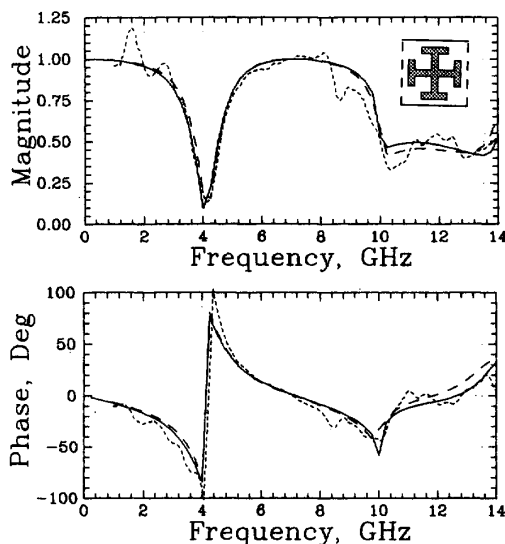


Figure 7: The transmission coefficient of an array of Jerusalem crosses. The solid line represents the full-wave theory presented here, the dashed line represents the theory presented in [9], the dotted line represents the measured results, and the unit cell of the structure is shown in the inset.